PCCP

FTIR spectroscopic characterization of a cationic lipid–DNA complex and its components

Walter Pohle,*[a] Carsten Selle,[b] Dorit R. Gauger,[a] Roman Zantl,[c] Franck Artzner[d] and Joachim O. Rädler[c]

[a] *Institute of Molecular Biology, Friedrich-Schiller University Jena, Winzerlaer str. 10, D-07745 Jena, Germany. E-mail: wapo@molebio.uni-jena.de*
[b] *Institute of Experimental Physics I, University of Leipzig, D-04103 Leipzig, Germany*
[c] *Technical University of Munich, Physics Department E22, D-85748 Garching, Germany*
[d] *Faculte de Pharmacie, URA 1218, CNRS, F-92296 Chatenay-Malabry Cedex, France*

Received 16th May 2000, Accepted 24th July 2000
First published as an Advance Article on the web 4th September 2000

FTIR spectroscopy is used to study structural aspects of ternary complexes formed by the cationic lipid dimyristoyltrimethylammoniumpropane (DMTAP), the zwitterionic lipid dimyristoylphosphatidylcholine (DMPC), and deoxyribonucleic acid (DNA). Spectra of the single components are compared with those obtained for both equimolar DMPC–DMTAP mixture and lipid–DNA complex. The IR spectra of mixed lipid–DNA phases are strongly dominated by the lipidic absorption bands. This allows one to easily monitor, in particular, the thermotropic phase behaviour of lipid within the complex. The IR spectra of DNA intercalated between cationic lipid bilayers are determined by subtracting corresponding pure lipid spectra from lipid–DNA complex spectra. These difference spectra indicate deviations of lipid–associated DNA from B-form DNA. Furthermore, two additional water bands arise at positions different from those known for lipid- and DNA-bound water which are indicative of two distinct states of hydration in lipid–DNA complexes. The pure lipid DMTAP exhibits unusual spectroscopic features at the temperature of chain melting, T_m, near 53 °C, which are attributed to the existence of a crystalline, headgroup-interdigitated phase existing at temperatures below T_m, in accordance with X-ray diffraction and differential scanning calorimetry (DSC) data.

Introduction

Gene transfer by means of cationic liposome formulations has become a standard, easy-to-use technique in molecular biology. The procedure known as lipofection is based on the fact that aggregates of cationic lipid and plasmid DNA are capable of delivering nucleic acids into eucaryotic cells.[1] There is hope that some day cationic lipid systems which are sufficiently efficient and good-natured to allow their application in somatic gene therapy will be designed.[2,3] However, clinical progress is hampered by the fact that structure and transport properties of lipid–DNA aggregates under *in vivo* conditions are poorly understood. Clearly, different cationic lipids have widely different propensities as transfection agents. The basic understanding of lipofection is that liposomes composed of mixtures of cationic lipid and neutral phospholipid condense DNA into compact aggregates. These aggregates stick to cell surfaces and are taken up by endocytosis. Then the endosomes formed dissolve and release free plasmids into the cytosol, and eventually some plasmids will find their way into the nucleus.[4] In each of these intermediate steps, the physicochemical properties of the lipids determine the structure and the aggregation behaviour of the gene-delivery complex. Hence, during the last years much attention has been given to molecular aspects of lipid–DNA complexes. In particular, the structure of lipid–DNA aggregates has been investigated for some exemplary lipid systems.[5–7] X-ray and neutron scattering elucidated an intriguing molecular arrangement of alternating layers of cationic lipid membranes and tightly packed liquid-crystalline DNA strands.[5,8] Alternatively, hexagonal phases were found.[9] Electron microscopy studies revealed morphological features,[10] and theoretical approaches have successfully rationalized interpretations of experimental data.[11,12] Spectroscopic methods well proven in lipid research, above all NMR spectroscopy, have also been used to explore DNA–lipid interactions.[13,14] A large positive surface potential of cationic lipids was revealed with the aid of a fluorescent probe combined with Gouy–Chapman theory.[15] The conformation of DNA in lipid complexes was examined by CD spectroscopy.[15,16] Another widely used technique that is powerful for examining lipid systems is FTIR spectroscopy which gives information, particularly, on a submolecular level[17–21] and, moreover, can reveal aspects of the molecular geometry if polarized light is applied onto oriented samples.[22,23] This method along with linear dichroism has also been frequently employed to study nucleic acids,[24–27] but so far not for lipid–DNA complexes except for work dealing with model systems.[28,29]

We report here on a FTIR spectroscopic study of a ternary complex consisting of calf-thymus NaDNA, DMPC and DMTAP. The lipid structures are schematically drawn in Fig. 1. The system DMTAP–DMPC–DNA was chosen because its thermotropic phase behaviour has already been largely characterized by us using DSC and X-ray scattering.[30,31] FTIR spectroscopy is promising to add some structural aspects to the current picture that has resulted from the essentially integral data obtained by DSC and X-ray scattering. Moreover, DMPC as one of the "classical" phospholipids has been extensively characterized by IR spectroscopy,[18,22,32-34] in contrast to DMTAP. The cationic lipid DMTAP turned out to exhibit some peculiar features. Regarded in conjunction with DSC and X-ray data, the IR spectroscopic results gave

 DOI: 10.1039/b003898i

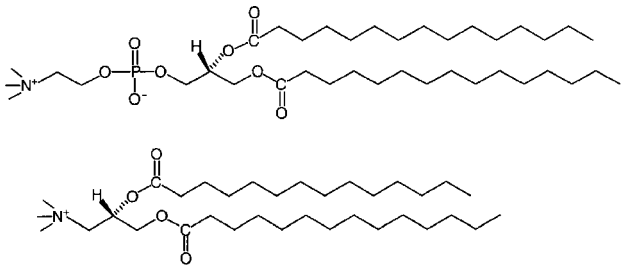

Fig. 1 Chemical structures of DMPC and DMTAP (below).

rise to an instructive picture of the unusual phase properties of DMTAP which may have some meaning for cationic lipids in general.

A further important question to be addressed by FTIR spectroscopy is the role of hydration. The state of hydration is intriguing since lipid–DNA aggregates are, according to the current models, so tightly packed that the amount of water entrapped within them should be rather limited, as can be derived from the membrane–DNA separation spacings known from structural X-ray work. Moreover, electrostatics demand, and experiments prove, that the counterions due to both DMTAP and DNA are entirely released from the complex.[35] Hence, the lipid–DNA aggregates are macromolecular salts, where the hydration state might deviate from that in the isolated components.

The paper is structured as follows. We firstly present data on purely lipidic systems and discuss their thermotropic phase behaviour. In the second part, we deal with the ternary cationic-lipid–helper-lipid–DNA complexes and discuss, in particular, the difference spectra of lipid-associated DNA.

Materials and methods

Materials

DMPC (1,2-dimyristoyl-*sn*-3-phosphatidylcholine) and DMTAP (1,2-dimyristoyl-3-trimethylammoniumpropane chloride) were purchased from Avanti Polar Lipids (Birmingham, AL, USA) in chloroform (purity 99 + %) and used without further purification. The sodium salt of calf-thymus DNA was obtained from Sigma (Deisenhofen, Germany).

X-ray diffraction and DSC

DMPC (35 mmol) and DMTAP (35 mmol) were mixed in chloroform. The solvent was removed under a nitrogen stream followed by desiccation for 20 h under vacuum. The dry lipid film was then hydrated with Millipore water to a total concentration of 50 (mg lipid) (ml water)$^{-1}$ at an elevated temperature of 60 °C. The lipid suspensions were vortexed and sonicated to clarity at 60 °C using a tip sonicator in order to form small unilamellar vesicles (SUV). The liposome suspensions were placed in 1 mm quartz capillaries for X-ray scattering or directly into a differential scanning calorimeter (VP-DSC, MicroCal, Northampton, MA, USA).

Lipid–DNA samples were mixed at charge neutral ratios and annealed by heating above the chain-melting transition temperature with subsequent cooling several times. The instrumental set-up for X-ray diffraction was described in detail in ref. 31.

FTIR spectroscopy

Appropriate amounts of the dispersions of the lipids and the DNA–lipid complex prepared as described for the X-ray and DSC samples were squeezed between two CaF_2 windows which were then placed into a thermostatable liquid cell. The pathlength of the samples was adjusted to 6 μm with Teflon spacers. DNA was measured as an unoriented film under a high relative humidity of 98%, *cf.* ref. 25.

FTIR spectra were recorded at different temperatures by an IFS-66 spectrometer from Bruker (Karlsruhe, Germany) equipped with a shuttle device. Samples were measured against air dried by passing through an adsorber (Zander, Essen, Germany). Heating–cooling cycles were run, and the sample temperature was controlled by an external circulating water bath (PGW Medingen, Freital, Germany) and monitored *via* a thermocouple with an accuracy better than 0.2 °C. The temperature was varied in steps of 2 °C within suitable intervals chosen for the different specimens. Before starting each measurement, the sample was kept at the adjusted temperature for 10 min.

32 scans were co-added to yield each of the spectra at a resolution of 2 cm^{-1} using a zero-filling factor of 2. Data processing was carried out with the OPUS software package (Bruker) and the program GRAMS (Galactic Instruments, Salem, NH, USA) and further standard software. The wavenumber uncertainty is less than 0.1 cm^{-1}.

Results and discussion

Lipid systems

IR spectra of dispersions of the single lipids, DMPC and DMTAP, as well as of their binary 1 : 1 mixture were measured at different temperatures. To provide an illustration for recorded raw data, Fig. 2 shows the overall spectra of DMPC and DMTAP at two different temperatures, 29 and 58 °C, respectively, chosen to have the lipids under comparable conditions well above their main-transition temperatures (by about 5 °C, see below). DMTAP exhibits surprisingly substantial absorption in the range 1200–1250 cm^{-1} which is, usually in phospholipids, occupied mainly by the intense band due to the antisymmetric PO_2^- stretching mode (see *e.g.* Fig. 2(a) for DMPC). On the other hand, the range between 1050 and 1100 cm^{-1}, where the band due to the symmetric PO_2^- stretch emerges in phospholipids, is largely clean, thus demonstrating the absence of phosphate groups in DMTAP.

As for the single lipids, we will focus in the following more on DMTAP as DMPC has been widely characterized previously.[18,22,32–34] In Fig. 3, the spectral ranges around the *ν*CH and *ν*C=O modes of DMTAP measured at two different temperatures, about 50 and 55 °C, are shown in an extended version. The temperature increase between the measurement of these spectra leads to drastic changes in the spectral parameters, especially increases in the peak wavenumbers (positions) of the bands due to the $\nu_s CH_2$ and *ν*C=O modes, $\tilde{\nu}_s CH_2$ and $\tilde{\nu}$C=O, which are accompanied by changes in band absorb-

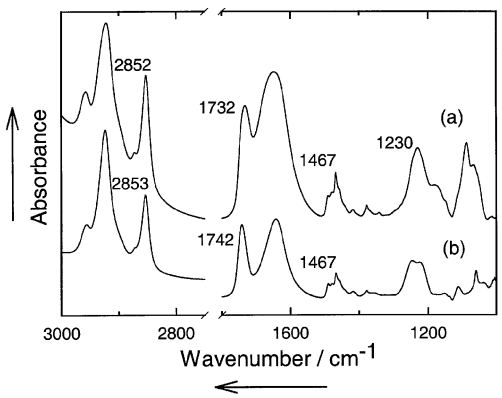

Fig. 2 Survey FTIR spectra of DMPC (above, (a)) and DMTAP (below, (b)) each obtained for a fully hydrated dispersion sandwiched between CaF_2 windows at temperatures of 29 and 58 °C, *i.e.* well (by about 5 °C) above the main-transition temperature in each case, *cf.* text and Fig. 4.

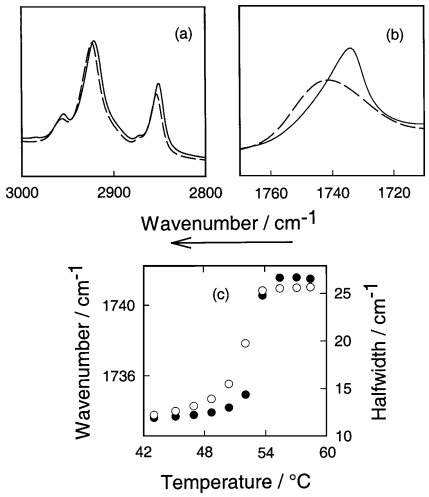

Fig. 3 FTIR spectra of DMTAP for two different temperatures of 50.4 (——) and 55.5 °C (– – –) which cover the ranges dominated by the bands due to C–H stretching (a) and C=O stretching vibrations (b); in (c), the wavenumbers (●) and the widths at half height (halfwidths, ○) of the *ν*C=O band were plotted *vs.* temperature.

ances and bandwidths. Upon heating DMTAP, the most striking changes are observed for *ν*C=O, namely strong increases in both frequency and full bandwidth at half height, or halfwidth for short. The graphs in Fig. 3(c) show that the changes in these two parameters are correlated with each other.

Some of the effects evident in Fig. 3 are quantified in Fig. 4 showing plots of the wavenumbers of the bands due to the $\nu_s CH_2$, $\delta_s CH_2$, *ν*C=O and $\nu_a PO_2^-$ vibrational modes *vs.* temperature for each of the lipid systems as well as for the lipid–DNA complex (the latter will be discussed in the next section). The spectra of the DMPC–DMTAP mixture and the lipid–DNA complex are given in Fig. 7(a) and (b), respectively, see below. Several of the dependences in Fig. 4 have in common steep frequency shifts at distinct temperatures which are marked by vertical lines through the four parts of Fig. 4. Looking for a clue to explain these distinct discontinuities, let us consider the findings in Fig. 4(a) first, since $\tilde{\nu}_s CH_2$ is the only one amongst the parameters always involved. The wavenumbers of the νCH_2 modes have been commonly used as a measure of the number or the portion of *gauche* conformers in hydrocarbon chains and, thus, as markers of their order state.[17–21] Accordingly, increases in one of these parameters, which are strong in terms of changes in the variable under study, are commonly taken as a reliable indicator of the chain-melting or main transition in lipid assemblies.[17–21] This phase transition can be triggered both thermally[17–21] and lyotropically, *i.e.* by increasing the water activity in the samples.[36,37]

Thus, the abrupt $\tilde{\nu}_s CH_2$ upward jumps registered between 2850 and 2852–2853 cm^{-1} in the present experiments evidence that chain-melting transitions proceed in the lipid aggregates formed in either of the samples. The main-transition temperatures, T_m, derived from the midpoints of these wavenumber shifts are about 24 °C for DMPC, in full agreement with the literature,[38] 41 °C for the lipid mixture and 53 °C for DMTAP. Fig. 5 shows DSC data of the three lipid samples. The T_m values revealed by DSC are largely coincident with those determined by IR spectroscopy. The main phase transition of DMTAP depends very critically on water concentration. DSC measurements in variously diluted DMTAP preparations exhibited obscure enthalpic transitions between 18 and 45 °C.[31,39] However, DMTAP studied at higher concentration (>20 wt.% lipid) showed a reproducible main transition at temperatures slightly above 50 °C.

From both the increase of $\tilde{\nu}_s CH_2$ and the DSC peak, the main transition of DMTAP is further characterized by a

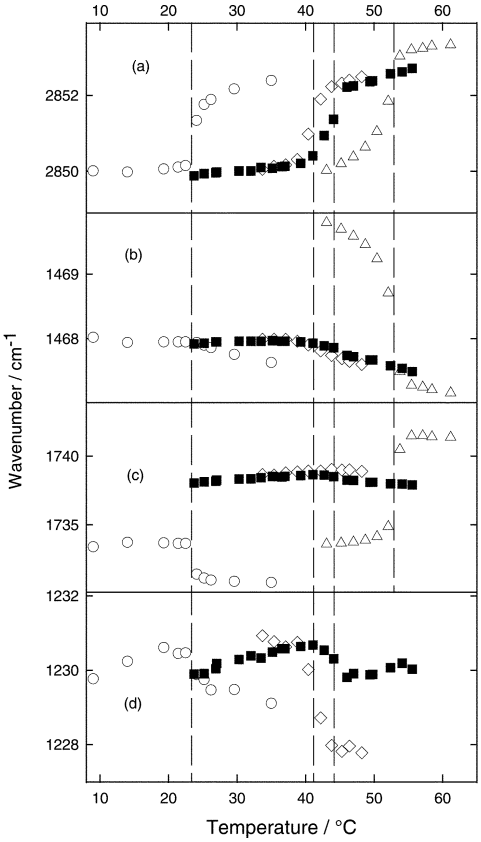

Fig. 4 Temperature dependence of the peak wavenumbers of selected absorption bands of DMPC (○), DMTAP (△), 1 : 1 DMPC–DMTAP mixture (◇) and DNA–lipid complex (■); the plots are for symmetric methylene stretch (a), methylene scissoring vibration (b), carbonyl stretch (c), and antisymmetric PO_2^- stretch (d). Striking correlated wavenumber shifts indicated by vertical broken lines occur for DMPC near 24 °C, for the lipid mixture near 41 °C, for the DNA complex near 44 °C and for DMTAP near 53 °C.

width clearly broader than in the other systems, as, for instance, DMPC (see Fig. 4(a), and Fig. 5(a) *vs.* Fig. 5(c)). The rise in the transition width of DMTAP is apparently mainly due to smaller slopes of $\tilde{\nu}_s CH_2$ and c_p in either of the onset regions and may reflect a certain loss in the cooperativity of the chain-melting process in the cationic lipid. This finding will be further discussed below. We suggest that the doublet structure of the DSC peak in DMTAP is due to inhomogeneities of the sample and does not reflect different phase transitions.

The high T_m difference between DMTAP and DMPC, almost 30 °C, implies an amazingly substantial stabilization of the solid (crystalline or gel) phase in the cationic lipid, which is unexpected in so far as *a priori* one also could have

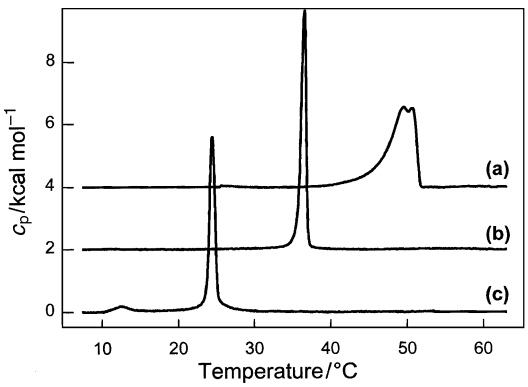

Fig. 5 Calorimetric scans of aqueous dispersions of DMTAP (a), DMPC–DMTAP mixture (b) and DMPC (c).

expected rather a destabilization of the solid phase due to the repulsive forces acting between positively charged headgroups. The T_m of about 41 °C found here for the equimolar DMPC–DMTAP mixture is somewhat higher than the 37–38 °C derived from our DSC measurements (see Fig. 5(b)). This discrepancy is probably caused by lower water contents of the samples used in IR spectroscopy, which were adjusted in order to create conditions more close to those pre-determined (by the preparation protocol) in the DNA–lipid complex. Lower water contents in IR spectroscopy have also the advantage that the interference from disturbing water absorption is simply less than in more dilute samples.

Among the relationships for the methylene scissoring–deformation vibration band depicted in Fig. 4(b), only the curve due to DMTAP displays a considerable change. This is a temperature-induced wavenumber downshift of ~ 3 cm^{-1} which is consistent with a transition from a state with triclinically packed acyl chains revealed by the magnitude of the band position of CH_2 scissoring-vibration mode of almost 1470 cm^{-1}, typical for crystalline phases,[18,19] to a disordered state of the chains to be expected for the lamellar liquid-crystalline phase, L_α. Interestingly, the courses of the curves due to δCH_2 and νCH_2 modes in Fig. 4(b) and (a) look exactly like reflected images, thus demonstrating that these two spectral features are indicative of the same structural event in DMTAP, that is, chain melting. The temperature dependences of the wavenumber of the band due to methylene scissoring-deformation vibration in the other two lipid systems are characterized also by systematic, but very small, frequency downshifts in the T_m range. The solid phases of DMPC as well as of the lipid mixture obviously lack the triclinical chain packing found for DMTAP.

The most intriguing results emerge from the $\tilde{\nu}$C=O data set shown in Fig. 4(c), see also Fig. 3(b) and (c). The values for DMPC undergo a distinct decrease by about 2.5 cm^{-1}; this is clearly due to the main transition as reported already several times in the literature[17–20,33,40] and generally ascribed to hydration of the carbonyl groups becoming stronger or more effective in the L_α phase, no matter whether that transition is triggered by temperature[17–20,33] or by hydration.[40] The explanation is plausible since the lamellar extension caused by chain melting is necessarily accompanied by an increase in the cross-sectional area of the lipid, thus facilitating the access of water molecules, particularly to the interfacial region where the carbonyl groups are situated near to the polar/apolar boundary. As confirmed by the results of quantum-chemical calculations, the bond order of carbonyl groups is indeed diminished upon hydrogen-bonding of water.[41] This finding is straightforward in explaining the decrease of $\tilde{\nu}$C=O observed usually upon hydration or chain melting. With this background, the considerable upshift of $\tilde{\nu}$C=O in DMTAP by nearly 8 cm^{-1}, which is unambiguously coupled with its main transition, seems to be counterintuitive. So it draws our attention to considerations arising from some experimental evidence that hydration may be a major but not the only factor determining the magnitude actually adopted by $\tilde{\nu}$C=O in a given system. Accordingly, this parameter can sensitively reflect implications arising from polarity and conformation (due to the torsional angles in the molecular subregion formed by the glycerol backbone and its ester bonding to acyl chains), also, and this is true particularly for dry or crystalline samples.[42–44] That is, the unusual temperature dependence of $\tilde{\nu}$C=O in DMTAP may indicate that the overall location of its carbonyl groups changes upon chain melting towards a less hydrated and/or less polar environment.

X-ray diffraction is the method of choice to obtain data that enable a better insight into the molecular organisation of the DMTAP–water system. Fig. 6 shows the results of X-ray diffraction on DMTAP–water aggregates. First, wide-angle X-ray scattering (WAXS) data clearly witness the existence of

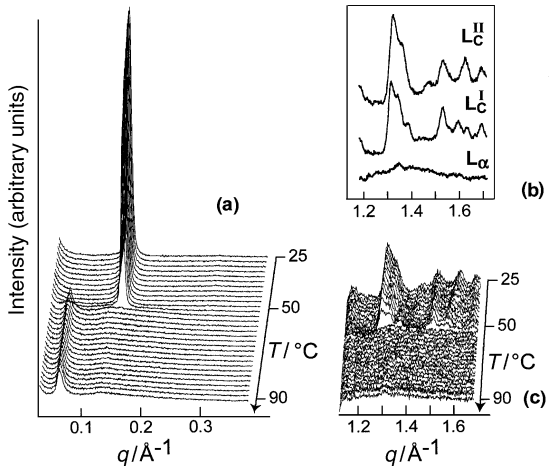

Fig. 6 Small-angle (a) and wide-angle (b, c) X-ray scattering of DMTAP–water mixtures (300 mg ml^{-1}) as a function of temperature; SAXS exhibits a transition from lamellar crystalline to swollen lamellar liquid-crystalline phase at a transition temperature near 53 °C. WAXS data confirm that this transition is associated with chain melting. Furthermore, a structural transition within the crystalline phase is found at about 40 °C.

two different crystalline (subgel) phases up to the T_m of 53 °C, as demonstrated by the patterns in Fig. 6(b) and (c). This is consistent with the IR spectroscopic finding of triclinically packed subcells typical for subgel phases arising from the respective data in Fig. 4(b). The small-angle X-ray scattering (SAXS) pattern (Fig. 6(a)) reveals, at $T < T_m$, a lamellar spacing of DMTAP of 4.2 nm, which is independent of the water content of the samples (data not shown). It is interesting to note that the absence of a second-order reflection in Fig. 6(a), usually not suppressed in L_c phases, is consistent with an electron density profile that misses a water layer between opposing headgroup layers. The repeat spacing of DMTAP is considerably smaller than the values around 5.5 nm found for DMPC under essentially similar conditions,[45–47] thus suggesting some degree of intercalation within the DMTAP layers. Hence, our data agree best with the idea of a headgroup-interdigitated crystalline phase present in hydrated DMTAP at temperatures below T_m. However, in a cationic lipid, such an arrangement demands inevitably the inclusion of counterions, chloride in this case, to shield the repulsion between the positively charged TAP residues. This necessity suggests a tight network of alternating TAP^+–Cl^- salt bridges will be formed in the headgroup region of crystalline DMTAP. The existence of salt bridges in cationic lipid systems was reported very recently.[15] Headgroup-interdigitated phases are well known for lipids with small headgroups, like DMPA, DMPE or $DODMA^+$ Br^-.[48] For instance, in phosphatidylethanolamines (PEs), the existence of a tight intermolecular headgroup network formed by long-lived hydrogen bonds and/or salt bridges between phosphate and ammonium groups is discussed[49–51] as being responsible for the remarkable stabilization of the solid phase of PEs compared to PCs, testified by a difference of the corresponding T_m values of about 20 °C.[38] The T_m difference between DMTAP and DMPC of even nearly 30 °C (*cf.* Fig. 4(a) and 5(a) and (c), and discussion above) is clear evidence that the solid-phase stabilizing headgroup-interdigitating network proposed for DMTAP is of a comparable or even higher strength than that typical for PE.

The spectroscopically unusual appearance of the carbonyl groups in crystalline DMTAP can be most easily rationalized by the influence of the strong electrostatic field proceeding from the postulated salt bridges and increasing the C=O polarity. More hypothetically, and less probably, it could also be evoked by the existence of a peculiar species of water mol-

ecules specifically hydrogen-bonded to these carbonyls which may be locked near the polar/apolar interface by the superficial trimethylammonium cation–chloride network. Due to the chain melting of DMTAP, those salt bridges would eventually be broken or at least significantly loosened, thus releasing and rearranging the array of carbonyl-bound water molecules. Both these alternative interpretations are in accord with the increase of the halfwidth of the νC=O band (Fig. 3(b) and (c)).

Once having passed the solid/liquid-crystalline phase transition, the lamellar repeat lengths of the DMTAP aggregates increase very strongly, to values near and above 10 nm, corresponding to the repeat distance of a fully swollen lamellar phase with a fraction of 20 wt.% of DMTAP.[52] Chain melting of DMTAP is obviously retarded as the broad transition ranges found by IR spectroscopy (*cf.* Fig. 4(a) and (b)) and DSC (see Fig. 5(a)) consistently indicate. This effect could emerge from the considerable stability presumably due to the TAP^+–Cl^- network which is formed in the headgroup region of DMTAP.

Returning to Fig. 4(c), the temperature dependence of $\tilde{\nu}$C=O in the lipid mixture is without any significant direction and represents a moderate position between the characteristics found for DMPC and DMTAP alone where these wavenumbers decrease and increase, respectively, in terms of chain melting. The figures of $\tilde{\nu}$C=O in the lipid mixture near 1739 cm^{-1} are relatively high and tend unequivocally towards the values typical for chain-melted DMTAP. This finding is consistent with poorly hydrated carbonyl groups of DMPC–DMTAP in a not particularly polar environment, which would disfavour the hypothetical assumption of the existence of another type of a (presumably more extended, less tight) salt-bridged headgroup network in the lipid mixture, even for its solid phase (*i.e.* below 41 °C in our case). However, an alternative explanation is that, in the headgroup region of the lipid mixture existing in the solid state, yet another type of "network" is formed between TAP^+ and the PO_2^- moieties from DMPC, as was concluded from the results of molecular dynamics simulations carried out for the DMPC–DMTAP system very recently.[11] Strong interactions of that kind may render the binding of water to carbonyl groups difficult.

Finally, in Fig. 4(d) the wavenumbers of $\nu_a PO_2^-$ were plotted *vs.* temperature. Figures from these plots are also given in Table 1 together with further data, see below. Whereas in DMPC only a weak respective significant change by $\sim$1 cm^{-1} could be observed, $\tilde{\nu}_a PO_2^-$ drops much more clearly in the lipid mixture by $\sim$3 cm^{-1}, correlated with the increase of $\tilde{\nu}CH_2$, *i.e.* with chain melting. For the L_α phase of the lipid mixture, this appears to reflect a hydration mode of the phosphate groups of DMPC which is more effective than in the solid phase existing in DMPC–DMTAP below 41 °C as well as in chain-melted DMPC (spectral effects of hydration on phosphate are discussed in more detail in the next section). This finding may indicate that strong TAP–PC headgroup interactions, as postulated above, occur particularly at $T < T_m$ and, thus, may account for a special property of cationic-lipid–helper-lipid mixtures.

Lipid–DNA complex

In Fig. 7(b), a survey spectrum of an isoelectric 1 : 1 : 1 complex of DMPC, DMTAP and DNA (with one cationic lipid per negatively charged DNA-phosphate) recorded at 33.5 °C is given. Comparison with the spectrum of the DMPC–DMTAP mixture measured at the same temperature, and shown in Fig. 7(a), reveals that the IR spectrum of the DNA complex is completely dominated by the features due to the lipidic part, and that significant DNA-specific features do not appear. This finding can be exploited to monitor structural characteristics of the lipid part in the complex without noticeable disturbance by DNA absorption.

The main transition in the lipid–DNA complex proceeding presumably between the so-called L_β^c and L_α^c phases (using the nomenclature introduced previously[5,31]) can be localized to occur near 44 °C, as elucidated by the plot of $\tilde{\nu}_s CH_2$ *vs.* temperature given in Fig. 4(a). Thus, DNA induces some increase in the main-transition temperature of the lipid in the complex, as previously observed by calorimetric investigations and explained by an electrostatic contribution due to the screening of the cationic bilayer by DNA.[31] The T_m of the lipid–DNA complex studied in the present work is again somewhat higher (by about 3 °C) than in the more diluted samples, with water

Table 1 Wavenumbers of the bands due to the antisymmetric stretching vibration, $\tilde{\nu}_a PO_2^-$, of lipid–DNA complex and related components

Sample	Conditions	$\tilde{\nu}_a PO_2^-$/cm^{-1}	$\Delta\tilde{\nu}_a PO_2^-$/$cm^{-1}$	Remarks/ref.
DMPC[a]	10 °C	1229.7		
	20 °C	1230.5	0.8	$\Delta\tilde{\nu}$ in solid phase
	26 °C	1229.3	−1.2	$\Delta\tilde{\nu}$ due to m.p.t.[b]
DMTAP-	34–39 °C	1230.8 ± 0.1		
DMPC[a](LM)	44–48 °C	1227.8 ± 0.1	−3.0 ± 0.2	$\Delta\tilde{\nu}$ due to m.p.t.[b]
LM-DNA[a]	25 °C	1229.9		
	41 °C	1230.7	0.8	$\Delta\tilde{\nu}$ in solid phase
	46 °C	1229.8	−0.9	$\Delta\tilde{\nu}$ due to m.p.t.[b]
	55 °C	1230.1	0.3	$\Delta\tilde{\nu}$ in l.c.[b] phase
DNA (Na)	Film, 98% RH	1223		B-Form
	Film, 75% RH	1235		A-Form
	Solution, 4.2% DNA, 20 °C	1223		B-Form[58]
	Solution, 4.2% DNA, 50 °C	1225		
DNA (Li)	Solution, 4.6% DNA, 20 °C	1223		C-Form[58]
	Solution, 4.6% DNA, 50 °C	1227		
	Film, 98% RH	1222		B-Form[59]
	59% RH	1227		C-Form[59]
DNA (Na)[c]	34–36 °C	1229.8 ± 0.4		
	40 °C	1231.7 ± 0.8	1.9 ± 1.2	This work
	42–48 °C	1232.1 ± 0.1	(0.4)[d]	This work

[a] All the samples containing lipids were dispersions, LM is for lipid mixture. [b] m.p.t. means main phase transition, l.c. liquid crystalline. [c] Lipid-associated DNA analysed from difference spectra. [d] This wavenumber shift is not significant.

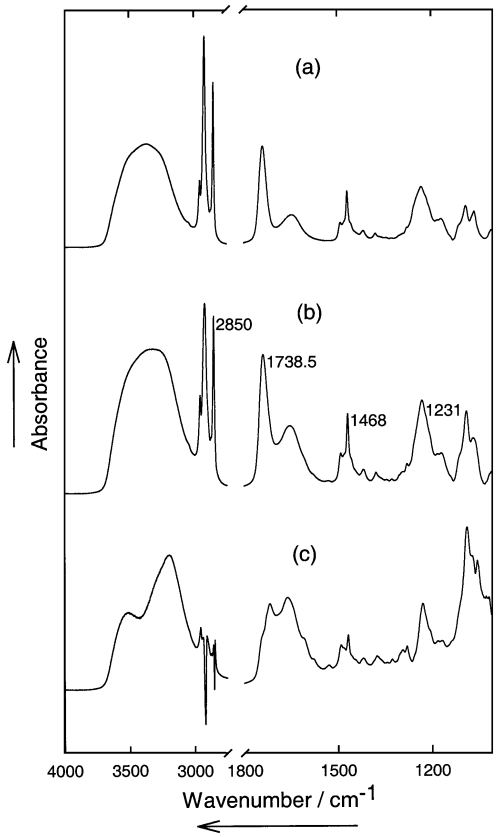

Fig. 7 Comparative overview of the IR spectra of an equimolar DMPC–DMTAP mixture (a) and a 1 : 1 : 1 ternary complex consisting of DMPC, DMTAP and DNA (b) obtained at 33.5 °C; the samples were dispersions. Spectrum (c) represents the difference of (b) − (a), *i.e.* lipid-bound DNA.

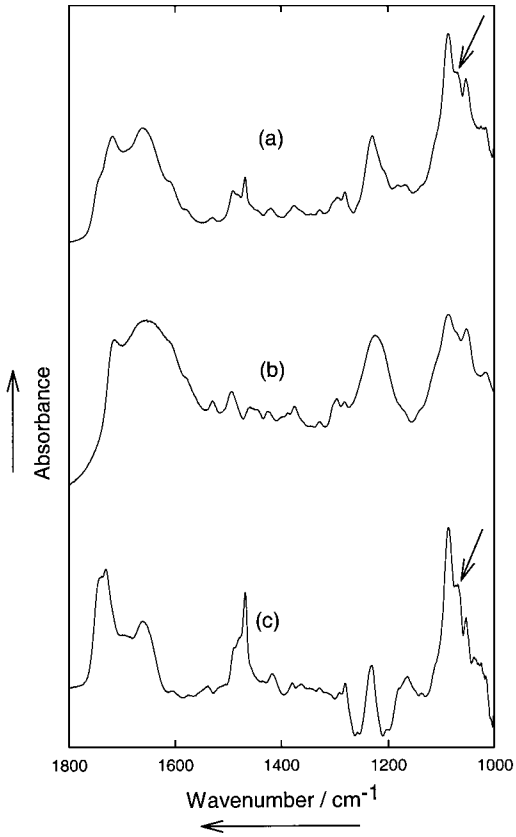

Fig. 8 IR spectra of lipid-bound DNA ((a) as in Fig. 7(c)) and of calf thymus NaDNA measured as an unoriented film at 27 °C and at a relative humidity of 98% (b), and double-difference spectrum (c) obtained if DNA is subtracted from lipid-bound DNA, *i.e.* spectra (a) and (b).

in large excess, used in DSC experiments, as already discussed for the lipid mixture (see above). The other dependences depicted for the lipid–DNA complex in Fig. 4(b)–(d) are rather unspectacular. The $\tilde{\nu}_a PO_2^-$ downshift observed in connection with chain melting is rather small, especially when compared to the lipid mixture (see last section and Table 1).

In an attempt to obtain spectral information for the DNA in the complex, we have subtracted lipid-mixture spectra from those of the lipid–DNA complex and obtained difference spectra due to lipid-bound DNA. Fig. 7(c) gives an example of such an IR spectrum for DNA, in this case embedded in the solid L_β^c phase (at 33.5 °C). The difference spectra are compared to the pattern typical for DNA, see Fig. 8(a) and (b). The IR spectra of DNA have been reported and widely discussed in the past, mostly for films investigated in terms of water activity.[24–27] Fig. 8(b) shows, as an example, a spectrum of a hydrated unoriented film of the calf-thymus NaDNA used for lipid complexation obtained at 98% relative humidity and exhibiting the IR spectroscopic markers for the B conformation predominating under these conditions.[24–27] DNA is polymorphic and can adopt, depending on its intrinsic primary structure and external conditions, a number of different forms called, *e.g.*, A, B, C, D or Z.[24–27] These forms can be classified into families of forms, for instance A and B families, which populate quite different regions of the conformational space.[53] Among the external parameters governing DNA conformation, hydrational state and ionic environment might be considered especially important.[54]

It should be mentioned that the procedure of spectral subtraction is by itself rather intricate. We defined a difference spectrum by a procedure leading selected calibration band(s) towards extinction, which results mostly in a residual dip-and-rise pattern of the calibration band(s) to be eliminated. Difference spectra generally should be regarded with some caution and as not equivalent to spectra obtained from direct measurement of absorption bands. The overall "DNA compatibility" emerging from the difference spectra of lipid-bound DNA as elucidated by a comparison of the spectra in Fig. 8(a) and (b), holding up even into spectral details, can be considered truly satisfactory. This gives us confidence to consider some of the spectral features of lipid-associated DNA in more detail.

The absorption in the 3000–4000 cm^{-1} range undoubtedly (since the subtraction processing was, intentionally, driven rather too far, as the slightly overcompensating dips in the spectral region around 3000 cm^{-1} in Fig. 7(c) testify) persisting in the difference spectra of lipid-bound DNA has to be ascribed to that peculiar water which forms a "surplus" portion present in the DNA complex in excess to the lipid mixture. Interestingly, the remaining νOH difference band

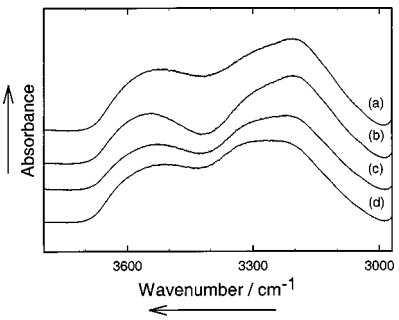

Fig. 9 IR difference spectra of lipid-associated DNA in the νOH region occupied by the O–H stretching-vibration band of water at different temperatures (°C) 33.5 (a), 42.5 (b), 44 (c) and 49 (d).

consists of two components with maxima around 3220 and 3530 cm^{-1} which occur not only at 33.5 °C (as in Fig. 7(c)) but also at the other temperatures in these measurements, as demonstrated by the spectra in Fig. 9. It should be mentioned that such spectral characteristics are not commonly observed for the *v*OH bands in either the IR spectra of hydrated lipids or of hydrated DNA as we have learned in our extensive studies carried out previously. Upon heating the lipid–DNA complex, the overall maximum of the low-frequency sub-band increases by $\sim$40 cm^{-1}, from about 3200 to 3240 cm^{-1}, which is obviously due to the rise of a high-frequency flank of that sub-band (see Fig. 9).

Although a comprehensive understanding of the apparently complex correlations existing between structural conditions (aggregations) in water and in aqueous systems and their spectroscopic response is currently largely not available, it may be legitimate to approach this problem on a rule-of-thumb level. So, the broad overall $\nu_{1,3}$OH water band around 3400 cm^{-1} can be assumed to result from a superposition of several underlying single bands representing a number of coexisting subpopulations of water aggregates differing in size and/or binding state. Accepting the existence of rough relationships, valid on an on-average basis, between the structural features due to the water in a given system and its general spectral parameters, it is reasonable to assume that the lower the wavenumber of the $\nu_{1,3}$OH water band the stronger the pertinent hydrogen bonds. Accordingly, the two resolved *v*OH sub-bands observed in lipid-associated DNA are to be assigned to different types of hydration water in the DNA–lipid complex, being distinguished by especially strong (3220 cm^{-1}) and weak (3530 cm^{-1}) hydrogen bonds. The position of the former sub-band is similar to that reported for *v*OH bands found in amorphous ice[55,56] or for water in highly hydrated DPPC cooled down to subzero temperatures.[34,57] This suggests that the 3220 cm^{-1} band can be attributed to highly immobilized water molecules, most probably involved in long-lived strong hydrogen bonds. It is most likely that they are located in the interfacial region between DNA double strands and lipid lamellae and form bifurcated bridges between the DNA backbone and lipid headgroups. The unstriking response of the IR bands due to the real or putative water-binding lipid sites (Fig. 4) does not contradict the idea of a bidentate mode of water binding since the latter would influence the involved water molecules themselves more strongly than these lipid groups. Moreover, it appears that this type of strongly bound water consists of two sub-species, as indicated by the structure of the contour of the 3220 cm^{-1} sub-band (see Fig. 9). It is plausible that the fraction of the subpopulation with the somewhat weaker H bonds increases with increasing temperature (Fig. 9).

The second type of very weakly H-bonded water, represented by the 3530 cm^{-1} sub-band, may consist of molecules or aggregates which are "left over" to accommodate to some "interstitial space" set between adjacent lipid bilayers on the one hand and DNA columns on the other. These water molecules are driven to fill the so-defined "interstices" in order to prevent them from remaining energetically unfavourable voids. Due to the volumes of these interstices, dictated by the overall geometry in the complex, unsuitable steric constraints may emerge for the water aggregates, resulting in a breakage of the (more) regular structures, which would be adopted in bulk water under the same thermodynamic conditions, and, eventually, in the formation of a sort of largely unordered, "entropic" water. These two different hypothetical water species which represent a peculiarity of the lipid–DNA complex are schematically illustrated in Fig. 10 and marked by (a) and (b) for strongly and weakly bound water.

In Table 1, peak wavenumbers of the $\nu_a PO_2^-$ band, $\tilde{\nu}_a PO_2^-$, of several of the systems related to the lipid–DNA complex are gathered. This parameter has been proven to very

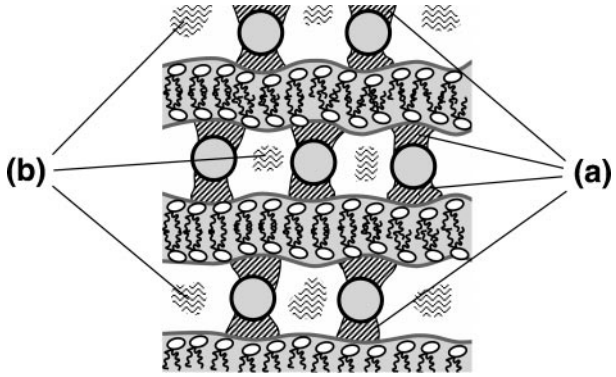

Fig. 10 Schematic drawing of a lamellar lipid–DNA complex highlighting the regions of the two hypothetical different states of hydration as suggested by the appearance of two particular IR absorption bands of water in the difference spectra of DNA incorporated in a DMTAP–DMPC complex (as in Fig. 7(c)). The boundary-water (dark-shaded (a), between DNA columns (symbolized by circles) and lipid layers is expected to be differently structured from the water in the interstices (light-shaded, (b)).

sensitively reflect environmental influences and/or structural changes in relevant biomolecules[60,61] which are sometimes difficult to distinguish. In lipids, it is indicative of both hydration effects, see ref. 36 and 41 and papers cited therein, and phase transitions.[21,37,62] As for DNA, $\tilde{\nu}_a PO_2^-$ depends on hydration as well as on conformation, as exemplarily shown in ref. 59 where also the observed hydration-dependent downshift is rationalized as originating from hydrogen bonding of water for the first time by the results of quantum-chemical calculations. For each of the lipid systems studied here, a significant decrease of $\tilde{\nu}_a PO_2^-$ occurring in terms of chain melting could be observed, which is by far the most pronounced in the lipid mixture (see above, Fig. 4(d)). This results in an overall tendency of the $\tilde{\nu}_a PO_2^-$ values to decrease if the whole temperature ranges studied are considered, at least for the samples containing only lipids. Only the values for the lipid–DNA complex remain approximately constant on balance. This becomes plausible if one regards $\tilde{\nu}_a PO_2^-$ for the lipid-bound DNA, since here a significant net increase by more than 2 cm^{-1} is obtained if temperature is raised. Heating DNA in solution enhances this parameter, too, independently of whether Na^+ or Li^+ were present as counterions.[58] This is a strong argument for believing that the band around 1230 cm^{-1} remaining in the difference spectra of lipid-associated DNA is actually due to DNA. That assignment is further corroborated by the absence of any $\tilde{\nu}_a PO_2^-$ decrease in the region around 44 °C where the lipids in the complex melt. The position of this difference band around 1230 cm^{-1} is rather different from that in the classical B form (usually 1222–1223 cm^{-1}) and tends rather to the magnitude characteristic of A-DNA (Table 1). However, C-DNA is also a candidate to exhibit somewhat larger figures for $\tilde{\nu}_a PO_2^-$.[58,59] The absorption near 1070 cm^{-1} arising in the difference spectra of DNA as a shoulder of the $\nu_s PO_2^-$ band (marked by the arrows in Fig. 8) can be attributed to the C form as we have previously observed in oriented films of LiDNA (unpublished data) and as is visible also in the spectrum of LiDNA in solution shown in Fig. 4 of ref. 58. Indications for C-DNA formed at least partly from B-DNA upon complexation with lipids were also found in previous CD measurements.[15,16] Nevertheless, the absolute figures for $\tilde{\nu}_a PO_2$ larger than 1230 cm^{-1} obtained for lipid-bound DNA (Table 1) are beyond the range of values typical for B- and C-DNA. This suggests that the surrounding lipids are able to induce some part of the incorporated DNA to adopt a structure towards the A form. The occurrence of coexisting conformations of a different type or of non-canonical conformations showing "intermediate"

structural features is probably rather the rule than the exception for DNA involved in complex systems, as several relevant examples of DNA–protein complexes document.[63–65]

The most striking feature in the "double-difference" spectra obtained by subtracting pure-DNA spectra from lipid-bound-DNA spectra is the remaining strong absorption of the band due to the symmetric PO_2^- stretching vibration, $\nu_s PO_2^-$, near 1090 cm^{-1} (see Fig. 8(c)) for an example). In this instance, the $\nu_a PO_2^-$ band intensity has been taken as the calibration band for the subtraction process. The weaker absorptions near 1730 and 1470 cm^{-1} also present are probably due to uncompensated lipid arising here even more clearly than in the difference spectra in Fig. 7(c). In previous studies, the intensity of the $\nu_s PO_2^-$ band has been demonstrated to depend on the electrostatics in the surroundings of the phosphate groups more clearly than is the case for its antisymmetric counterpart. The increasing influence of charged counterions resulted in significant enlargements of this band which became evident for both sodium ions in low-hydrated DNA films (unpublished data) and positively charged polypeptides.[66] This preliminary finding is consistent with the interpretation that cationic lipids, like DMTAP, can affect DNA *via* electrostatic attraction more than the diffuse cloud of small counterions in DNA solutions, the latter as it was described by the theory of Manning.[67]

Conclusion

A lipid–DNA complex with model character consisting of cationic DMTAP, DMPC as a helper lipid, and common calf-thymus DNA was investigated by FTIR spectroscopy. Comparative measurements were performed for the lipid components and hydrated DNA. We demonstrated that IR spectroscopy, which so far has not been used in physicochemical studies of such complexes, has considerable potential for exploring aspects of the lipid phase behaviour and the conformation of DNA not only for the components, but also in the lipid–DNA complex. From the difference spectra of lipid-associated DNA, tentative conclusions could be drawn with respect to both the hydration of the complex and the conformation of DNA. The νOH band of water is split into two components which are indicative of the coexistence of two separated water populations distinguished by hydrogen bonds of very different strengths. As for the conformation of DNA, the signatures of both C-DNA and A-DNA could be found in contrast to the B-form predominating in pure DNA under the same conditions. This is an indication that lipids may influence the properties of the nucleic acids to be transfected in gene therapy at least intermediately. *Vice versa*, DNA affects the phase behaviour of the lipid mixture used for coating it, too. The stabilization of solid phases of the involved lipids by DNA, already observed in previous studies with other methodology, could be confirmed by IR spectroscopic data.

Moreover, interesting novel features concerning lipid systems as used in transfection were elucidated by utilizing specific strengths of IR spectroscopy. For instance, especially strong changes in hydration and/or conformation are indicated for the phosphate groups of DMPC in the DMTAP–DMPC mixture in the course of chain melting. The main transition of DMTAP was shifted considerably to higher temperatures (by about 30 °C) compared to its analogue DMPC. This stabilisation of the solid state of DMTAP together with the unusual spectral behaviour of the carbonyl groups was interpreted in terms of a headgroup-interdigitated crystalline phase. The latter was confirmed by X-ray diffraction data and is most probably accompanied by the formation of salt bridges which obviously influence the polarity at the polar/apolar interface. Upon chain melting, this headgroup order is broken, thus leading to a decline in electrostatic effects exerted on carbonyl groups in the liquid-crystalline phase. It appears that cationic lipids constitute a class of amphiphiles with properties extremely interesting also in a heuristic sense.

Acknowledgements

The financial support given by Deutsche Forschungsgemeinschaft in the frame of SFB 197, subproject B10 (W.P., C.S. and D.R.G.) and by Bundesministerium fuer Bildung und Forschung, grant 03SA5TU10 is gratefully acknowledged. Furthermore, the authors are indebted to Dr. Gert Rapp for the help in obtaining data for Fig. 6 and to Prof. Hartmut Fritzsche for valuable discussions.

References

1 P. L. Felgner, T. R. Gadek, M. Holm, R. Roman, H. W. Chan, M. Wenz, J. P. Northrop, G. M. Ringold and M. Danielson, *Proc. Natl. Acad. Sci. USA*, 1987, **84**, 7413.
2 D. D. Lasic, *Liposomes in Gene Delivery*, CRC Press, Boca Raton, 1997.
3 D. Miller, *Angew. Chem.*, 1998, **110**, 1862.
4 J. Zabner, A. J. Fasbender, T. Moninger, K. A. Poellinger and M. J. Welsh, *J. Biol. Chem.*, 1995, **270**, 18997.
5 J. O. Rädler, I. Koltover, T. Salditt and C. R. Safinya, *Science*, 1997, **275**, 810.
6 D. D. Lasic, H. Strey, M. C. A. Stuart, R. Podgornik and P. M. Frederik, *J. Am. Chem. Soc.*, 1997, **119**, 832.
7 T. Boukhnikachvili, O. Aguerre-Chariol, M. Airiau, S. Lesieur, M. Ollivon and J. Vacus, *FEBS Lett.*, 1997, **409**, 188.
8 T. Salditt, I. Koltover, J. O. Rädler and C. R. Safinya, *Phys. Rev. Lett.*, 1997, **79**, 2582.
9 I. Koltover, T. Salditt, J. O. Rädler and C. R. Safinya, *Science*, 1998, **281**, 78.
10 S. Huebner, B. J. Battersby, R. Grimm and G. Cevc, *Biophys. J.*, 1999, **76**, 3158.
11 S. Bandyopadhyay, M. Tarek and M. L. Klein, *J. Phys. Chem. B*, 1999, **103**, 10075.
12 S. May, D. Harries and A. Ben-Shaul, *Biophys. J.*, 2000, **78**, 1681.
13 P. Mitrakos and P. M. Macdonald, *Biochemistry*, 1996, **35**, 16714.
14 K. W. Mok and P. R. Cullis, *Biophys. J.*, 1997, **73**, 2534.
15 N. J. Zuidam and Y. Barenholz, *Int. J. Pharm.*, 1999, **183**, 43.
16 K. Tanaka and Y. Okahata, *J. Am. Chem. Soc.*, 1996, **118**, 10679.
17 H. L. Casal and H. H. Mantsch, *Biochim. Biophys. Acta*, 1984, **779**, 381.
18 A. Blume, W. Hübner and G. Messner, *Biochemistry*, 1988, **27**, 8239.
19 H. H. Mantsch and R. N. McElhaney, *J. Mol. Struct.*, 1990, **217**, 347.
20 M. Jackson and H. H. Mantsch, *Spectrochim. Acta Rev.*, 1993, **15**, 53.
21 R. N. A. H. Lewis and R. N. McElhaney, in *Infrared Spectroscopy of Biomolecules*, ed. H. H. Mantsch and D. Chapman, Wiley-Liss, New York, 1996, p. 159.
22 W. Hübner and H. H. Mantsch, *Biophys. J.*, 1991, **59**, 1261.
23 L. K. Tamm and S. A. Tatulian, *Quart. Rev. Biophys.*, 1997, **30**, 365.
24 J. Pilet and J. Brahms, *Biopolymers*, 1973, **12**, 387.
25 W. Pohle, V. B. Zhurkin and H. Fritzsche, *Biopolymers*, 1984, **23**, 2603.
26 W. Pohle and H. Fritzsche, *J. Mol. Struct.*, 1990, **219**, 341.
27 J. Liquier and E. Taillandier, in ref. 21, p. 131.
28 G. B. Sukhorukov, L. A. Feigin, M. M. Montrel and B. I. Sukhorukov, *Thin Solid Films*, 1995, **259**, 79.
29 V. I. Sukhorukov, M. M. Montrel, G. B. Sukhorukov and L. I. Shabarchina, *Biophysics*, 1994, **39**, 273.
30 F. Artzner, R. Zantl, G. Rapp and J. O. Rädler, *Phys. Rev. Lett.*, 1998, **81**, 5015.
31 R. Zantl, L. Baicu, F. Artzner, I. Sprenger, G. Rapp and J. O. Rädler, *J. Phys. Chem. B*, 1999, **103**, 10300.
32 A. Mellier, *Chem. Phys. Lipids*, 1989, **51**, 23.
33 J. Ter-Minassian-Saraga, E. Okamura, J. Umemura and T. Takenaka, *Biochim. Biophys. Acta*, 1988, **946**, 417.
34 J. Grdadolnik, J. Kidric and D. Hadzi, *J. Mol. Struct.*, 1994, **322**, 93.
35 K. Wagner, D. Harries, S. May, V. Kahl, J. O. Rädler and A. Ben-Shaul, *Langmuir*, 2000, **16**, 303.
36 W. Pohle, C. Selle, H. Fritzsche and H. Binder, *Biospectroscopy*, 1998, **4**, 267.

37 C. Selle, W. Pohle and H. Fritzsche, *J. Mol. Struct*., 1999, **401**, 480.
38 M. Caffrey, *Lipid Thermotropic Phase Transitions*, National Institute of Standards and Technology, Gaithersburg, 1993.
39 J. R. Silvius, *Biochim. Biophys. Acta*, 1991, **1070**, 51.
40 C. Selle and W. Pohle, *Biospectroscopy*, 1998, **4**, 281.
41 W. Pohle, C. Selle, H. Fritzsche and M. Bohl, *J. Mol. Struct*., 1997, **408/409**, 273.
42 I. W. Levin, E. Mushayakarara and R. Bittman, *J. Raman Spectrosc*., 1982, **13**, 231.
43 R. N. A. H. Lewis, R. N. McElhaney, W. Pohle and H. H. Mantsch, *Biophys. J*., 1994, **67**, 2367.
44 C. Selle, Thesis, Jena, 1999.
45 M. J. Janiak, D. M. Small and G. G. Shipley, *J. Biol. Chem*., 1979, **254**, 6068.
46 R. H. Pearson and I. Pascher, *Nature*, 1979, **281**, 499.
47 E. B. Sirota, G. S. Smith, C. R. Safinya, R. J. Plano and N. A. Clark, *Science*, 1988, **242**, 1406.
48 I. Pascher, M. Lundmark, P.-G. Nyholm and S. Sundell, *Biochim. Biophys. Acta*, 1992, **1113**, 339.
49 H. Hauser, I. Pascher, R. H. Pearson and S. Sundell, *Biochim. Biophys. Acta*, 1981, **650**, 21.
50 J. M. Boggs, *Biochim. Biophys. Acta*, 1987, **906**, 353.
51 R. N. A. H. Lewis and R. N. McElhaney, *Biophys. J*., 1993, **64**, 1081.
52 D. Roux and C. R. J. Safinya, *Physique France*, 1988, **49**, 307.
53 V. B. Zhurkin, Yu. P. Lysov and V. I. Ivanov, *Biopolymers*, 1978, **17**, 377.
54 W. Pohle and M. Bohl, *Biospectroscopy*, 1995, **1**, 101.
55 E. Mayer, *J. Phys. Chem*., 1985, **89**, 3474.
56 G. Nielson and S. A. Rice, *J. Chem. Phys*., 1983, **78**, 4824.
57 E. Okamura, J. Umemura and T. Takenaka, *Vib. Spectrosc*., 1991, **2**, 95.
58 H. Fabian, *Stud. Biophys*., 1978, **72**, 99.
59 W. Pohle and M. Bohl, *Stud. Biophys*., 1987, **122**, 113.
60 W. Pohle, *J. Mol. Struct*., 1990, **219**, 281.
61 W. Pohle, M. Bohl and H. Böhlig, *J. Mol. Struct*., 1991, **242**, 333.
62 R. N. A. H. Lewis, W. Pohle and R. N. McElhaney, *Biophys. J*., 1996, **70**, 2736.
63 Y. Kim, J. H. Geiger, S. Hahn and P. B. Sigler, *Nature*, 1993, **365**, 512.
64 G. Guzikevich-Duerstein and Z. Shakked, *Nat. Struct. Biol*., 1996, **3**, 32.
65 R. E. Dickerson, *Nucleic Acids Res*., 1998, **26**, 1906.
66 S. Böhm, personal communication.
67 G. S. Manning, *Quart. Rev. Biophys*., 1978, **2**, 179.